



# Maximum Pressure Evaluation during Expulsion of Entrapped Air from Pressurized Pipelines

D. M. Bucur<sup>1</sup>, G. Dunca<sup>1†</sup> and M. J. Cervantes<sup>2,3</sup>

<sup>1</sup> University POLITEHNICA of Bucharest, Romania

<sup>2</sup> Luleå University of Technology, Luleå, Sweden

<sup>3</sup> Norwegian University of Science and Technology, Trondheim, Norway

†Corresponding Author Email: [georgianadunca@yahoo.co.uk](mailto:georgianadunca@yahoo.co.uk)

(Received March 15, 2016; accepted September 27, 2016)

## ABSTRACT

Pressurized pipeline systems may have a wide operating regime. This paper presents the experimental analysis of the transient flow in a horizontal pipe containing an air pocket, which allows the ventilation of the air after the pressurization of the hydraulic system, through an orifice placed at the downstream end. The measurements are made on a laboratory set-up, for different supply pressures and various geometries of water column length, air pocket and expulsion orifice diameter. Dimensional analysis is carried out in order to determine a relation between the parameters influencing the maximum pressure value. A two equations model is obtained and a criterion is established for their use. The equations are validated with experimental data from the present laboratory set-up and with other data available in the literature. The results presented as non-dimensional quantities variations show a good agreement with the previous experimental and analytical researches.

**Keywords:** Air expulsion; Air pocket; Pressure wave speed; Transient; Dimensionless analysis.

## NOMENCLATURE

$c$	pressure wave speed	$p_0$	atmospheric pressure
$d$	orifice diameter	$p_{max}$	maximum pressure
$D$	pipe diameter	$p_R$	supply pressure
$E$	Young modulus	$R$	Reynolds number
$e$	wall thickness	$t$	time
$f$	generic function	$v$	flow velocity
$K$	bulk modulus		
$k$	characteristic constant of the set-up	$\pi$	PI theorem parameters
$krit$	selection criterion	$\mu$	water dynamic viscosity
$L_a$	air pocket length	$\rho$	water density
$L_t$	pipe length	$\alpha$	relative air pocket length
$L_w$	water column length	$\beta, \gamma, \delta, \varepsilon$	coefficients of PI parameters
$p$	pressure		

## 1. INTRODUCTION

Hydraulic energy represents today the most important source of energy that can be stored. The storage technique consists in pumped hydroelectric facilities which can operate either as power generators or as power consumers, according to the grid requirements. As the energy market is very dynamic, these facilities operation includes many starts and stops, change of load and even change of

flow direction. Hydroelectric sites are very complex structures with reservoirs, surge tanks and secondary intakes. The sudden manoeuvres of the hydro units lead to changes of flow rate and can cause the entrapment of large air pockets occupying the entire cross section of the pipe, which are compressed and moved together with the water column (Tatu 1999, Gjerde 2009).

The consequences of entrapped air pockets are several. The presence of air can decrease the

hydraulic capacity of the pipe, affect the flow field (including turbulence, wall-shear), modify the pressure surges during transients and change the bulk properties of the fluid (density and elasticity) (Lauchlan *et al.*, 2005). If the water is mixed with air while passing through hydraulic machineries, their efficiency is reduced (Lauchlan *et al.*, 2005). Expulsion of air from the hydraulic systems can cause water hammer phenomenon, with damped or increased magnitude function of the air volume.

Still, depending on the ratio of the air volume to the water volume, the presence of air pockets can be favourable since having a cushioning effect. However, most of the times, entrapped large air pockets cause undesirable effects. The worst situations happen when the air is expelled from the system, causing important damages to the structures. Many incidents have been reported and analyzed in the literature; in some cases, the expulsion of a large quantity of air was so powerful that it blown up the concrete structures (EHG 1996; Tatu 1999; Zhou *et al.* 2004; Gjerde 2009; Lee 2005).

Recently, much work, both numerical and experimental, has been dedicated to analyse the high pressure surges caused by the presence of the air in the system (Zhou *et al.* 2004; Lee 2005; Lee *et al.* 2008; De Martino *et al.* 2008; Carlos *et al.* 2011) in order to determine the influence of initial pressure, water column length, air pocket volume and orifice diameter on pressure surge.

Several mathematical models were developed, with different degrees of complexity. Usually, the numerical models used are the elastic water model and the rigid column model. The first one considers the elasticity of both the water and pipe and is solved using the method of characteristics (MOC). The second one ignores the elasticity of both the water and pipe allowing shorter computational time and an easy implementation. Liou and Hunt (1996) formulated a model to describe the unsteady motion of a rigid water column filling an empty pipeline. They obtained the time histories of the length, velocity and pressure distribution along the water column. Izquierdo *et al.* (1999) presented a mathematical model used to obtain the maximum pressure that air pockets within a pipeline can cause on start-up, while Lee *et al.* (2008) developed a variable wave speed model to study the effects of air entrainment on pressure transients caused by a pump sudden stop.

Besides MOC or lumped inertia approaches, Volume of Fluid (VOF) is used for some time to simulate different multiphase flows (Cheng *et al.*, 2007, Pitorac *et al.* 2016). Liu and Zhou (2009) developed a 2D VOF model for the simulation of transient flow in pipe with entrapped air able to determine the displacement of air-water interface, pressure distribution and maximum pressure value. A 3D VOF model of a transitory flow without air expulsion was developed and validated with experimental data by Zhou *et al.* (2011). The results regarding the air pocket movement and pressure surge were in good agreement with experimental data.

Mathematical models developed and presented in literature are complicated to use. They involve complex mathematics and need detailed description of the set-ups parameters for the computation of the maximum pressure. Therefore, a simple and fast tool predicting the maximum pressure with minimum information regarding geometric and hydraulic parameters may be useful in the early design stages or during operation of the hydraulic systems.

In the present paper, a mathematical model to determine the maximum pressure during transients with air expulsion is developed based on detailed experimental works. The main advantage of the proposed model is the easy implementation for various configurations and its accuracy despite taking into account few parameters. The pressure measurements were realized for a wide range of the geometrical characteristics relative to the pipe diameter: air content varying from 0.0554 to 0.4797 of total volume and relative orifice sizes in the range 0.076 to 0.374.

The model is obtained using dimensional analysis and consists in two equations. A criterion allows determining the use of the appropriate equation. The validation is performed both on current measurements and experimental data available in the literature (Zhou 2000, Lee 2005). In case of literature data validation, constants characteristics of the set-ups had to be introduced for fitting. Generally, the trend and most of the pressure values are well captured, the model being able to consider the influence of system configurations and operation conditions. The results can be useful in the assessment of unsteady pressures with expulsion of air following sudden manoeuvres of the gates within pressurized hydraulic systems, especially in relative large orifices range situations. Still due to the unknown characteristics constants of the set-ups, the model needs to be further investigated.

## 2. EXPERIMENTAL APPARATUS AND PROCEDURES

The investigations were made in the Hydro Equipment laboratory from University Politehnica of Bucharest, Romania, in a closed circuit set-up designed to create different configurations for air - water transient flows.

### 2.1 Experimental Setup

The experimental set-up consisted in a pressure tank, pipe with five butterfly valves, downstream tank, pump and compressor (Fig. 1). The pipe has a total length,  $L_t$ , of 10.11 m. The first 0.48 m of the pipe is made of polypropylene, while the rest of the pipe is made of transparent Plexiglas. The interior section of the pipe is circular with a 39 mm diameter,  $D$ , and the exterior section is rectangular ( $50 \times 50$  mm<sup>2</sup>) in order to achieve a high quality visualization of the process. The end of the pipe is provided with orifices having an inner diameter,  $d$ , ranging from 3 to 15mm.

The supply tank with the compressor are used at the

upstream end of the pipe and can supply pressure heads up to 10 bar (Fig. 1). The supply tank has a total volume of 200 l and the downstream tank, with 125 l, is used to collect the water. From the downstream tank the water is pumped back into the supply tank. This action takes place before the experiment. During the experiment, the pump is turned off.

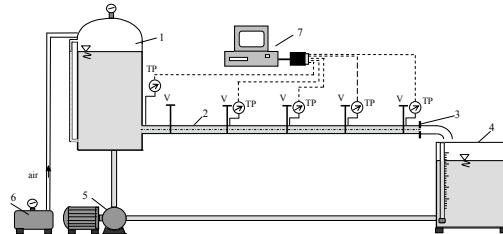


**Fig. 1. Experimental setup:** 1 – supply tank, 2 – pipe, 3 – orifice, 4 – downstream tank, 5 – pump, 6 – compressor, 7 – data acquisition system, V – fast opening valves, TP – pressure transducers.

The different air-water length configurations are realized with five pneumatically driven butterfly valves (V in Fig. 1) placed at 2.15 m from each other. The first valve is located 0.96 m downstream the supply tank and the last one 0.55 m upstream the pipe end (Fig. 2). The water column lengths that can be obtained are 9.57, 7.43 and 5.28 m. The valves closing/opening time depends on the pressure from the valves actuators pneumatic circuit. The pressure is supplied by the tank compressor, in a separated circuit. For the present setup, the air pressure is set at 4 bars, which corresponds to valves opening time of about 20 ms.

Five pressure taps are mounted on the top side of the pipe, 5.5 cm above the water surface. The first one (TP1) is placed close to the supply tank, on the polypropylene sector, while the other four are placed on the Plexiglas pipe. The distances from the supply tank to the pressure taps are 0.16, 3.20, 5.35, 7.50 and 9.65 m. Membrane-type pressure transducers with measuring range 0 – 40 bar, accuracy of 0.25%, repeatability 0.1% of full scale and 1 ms response time are used for the pressure measurements.

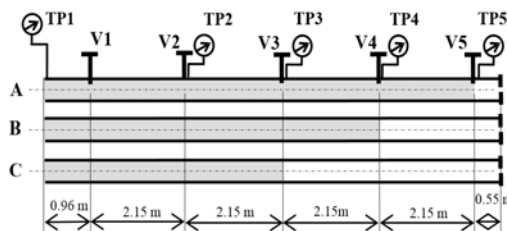


**Fig. 2. Pressure transducers arrangement related to air pocket initial length.**

The transducers are connected to a Keithley data acquisition board (KUSB-3100), which has an accuracy of 0.1%, resolution of 12 bit and a sampling rate of 50 kSa/s. The signal from the five

transducers is acquired simultaneously with a sampling frequency of 10 kHz during a 5 s period.

## 2.2 Procedures and Measurement Program

During the experiments, the pipe is first fully filled with water at the desired supply pressure. Then, depending on the length of the water column tested, one of the butterfly valves is closed and the downstream water is evacuated, setting the initial pressure in the air pocket at atmospheric value. The tests are conducted by opening fast the butterfly valve (within 20 ms). During the pipe filling process, the head of the supply tank decreases function of the orifice and air pocket sizes (up to a maximum of 10% from the initial supply pressure).

The pressure variations are simultaneously recorded with all five pressure transducers. Each test is repeated three times. The repeatability of the measurements shows a maximum peak pressure variation up to 13% for all situations, except for  $d/D = 0.2308$  when the variation reaches 36%. The pressure data is smoothed using the Savitzky-Golay method in Matlab for the graphical representation. This method preserves the width and amplitude of the signal (Schafer 2011). The evaluation, computation and modelling of maximum pressure is done without filtering the data.

Three configurations of water column and air pocket lengths are tested with five different supply pressures,  $p_R$ , ranging from 2 to 4 bars and five different orifices ranging from 3 to 15 mm (Table 1). These arrangements place one, two or three pressure transducers in the air pocket area (Fig. 2).

**Table 1 Experimental configurations**

Parameter	Test case		
	A	B	C
$\alpha$	0.0544	0.2671	0.4797
$p_R/p_0$	2; 2.5; 3; 3.5; 4		
$d/D$	0.076; 0.128; 0.179; 0.230; 0.374		

The relative supply pressure parameter,  $p_R/p_0$ , is the absolute value of the supply pressure,  $p_R$ , made dimensionless with the atmospheric pressure,  $p_0$ . The relative orifice size is expressed as the orifice diameter divided by the pipe diameter,  $d/D$ . An expression of relative air pocket size, related to the total length of the air pocket,  $L_a$ , and water column,  $L_w$ , is also used:

$$\alpha = \frac{L_a}{L_a + L_w} = \frac{L_a}{L_t} \quad (1)$$

## 3. EXPERIMENTAL RESULTS

determined by the supply tank pressure,  $p_R$ . Downstream the separation valve, the air pocket is at the atmospheric pressure,  $p_0$ . When the separation valve opens, the pressure difference between the water and air column accelerates the water column and compresses the air pocket to the end of the pipe.

Most of the initial air volume is vented through the orifice until the water column reaches the orifice at the downstream end of the pipe. Because the orifice is placed in the axis of the pipe, a part of the initial air pocket may remain captive above the orifice, at the top side of the pipe. This captive air quantity depends mainly on the orifice size and the supply pressure. In case of relatively small orifices, after reaching the downstream end of the pipe, the water column flow reverses, uncovering the orifice and allowing the trapped air to be vented or entrapping new air in the pipe, through the orifice. In case of larger orifices, the air is completely expelled and the phenomenon is similar to a sudden shock (water hammer). Still, the presence of entrapped air was observed in the pressure traces, but its influence over the pressure surges was important only in case of small orifice sizes.

### 3.1 Configuration A

In this configuration the air quantity is the smallest,  $\alpha = 0.0544$ , and it is expected a reduced cushioning effect. For the smaller orifices,  $d/D = 0.076$ ;  $0.128$ , a slight increase of the pressure in the air pocket was observed, before the impact of the water column with the downstream end of the pipe. This suggests that the air was compressed before the expulsion from the pipe. For the larger orifices,  $d/D = 0.179$ ;  $0.230$ ;  $0.374$  the compression was not present and the air was expelled immediately, the water hammer phenomenon being dominant. The influence of the orifice diameter presented in Fig. 3 for case A at 4 bar supply pressure, shows a significant decrease of the maximum pressure with the increase of the orifice size, after the value of  $d/D = 0.128$ .

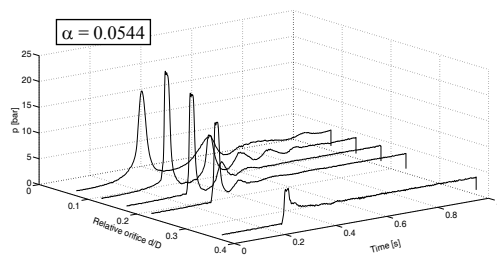


**Fig. 3. Orifice diameter influence over pressure at TP5, case A,  $p_R = 4$  bar.**

Figure 4 presents the pressure variation recorded by all sensors, for a supply pressure of 4 bar and a relative orifice size of  $0.128$ . At TP 2, 3 and 4 sections placed in the water column, the pressure recordings show the presence of acoustic effects immediately after opening the separation valve ( $t = 0.2$  second) and before water reaches the orifice ( $t = 0.5$  second). In the signal recorded by TP1, these effects are not present due to its proximity to the supply tank which acts as a buffer.

The pressure in the upstream tank determines the velocity of the water column, after the valve opening and thus influences the maximum pressure surge. In Fig. 5, the pressure variation recorded at TP5 is presented in configuration A for  $d/D = 0.128$

for three different values of the supply pressure. In this situation, the maximum surge pressure reaches up to six times the supply pressure in the air pocket section.

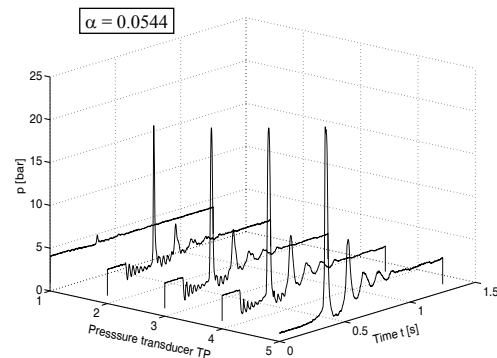


**Fig. 4. Pressure variation in time for case A,  $p_R = 4$  bar,  $d/D = 0.128$ .**

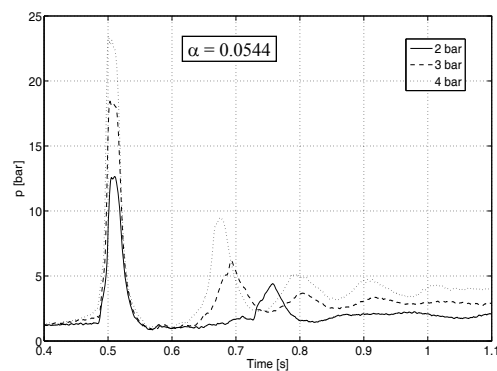


**Fig. 5. Supply pressure influence over the pressure variation at TP5, case A,  $d/D = 0.128$ .**

### 3.2 Configuration B

The relative air pocket length of this configuration has  $\alpha = 0.2671$  and two pressure transducers are placed in the air pocket (TP 4 and 5). The air pocket compression also for the small orifices ( $d/D = 0.076$ ;  $0.128$ ) is more obvious than in the previous case. For the larger orifices ( $d/D = 0.179$ ;  $0.230$ ;  $0.374$ ), the air compression is strongly decreased with the increase of the orifice size, the air pocket being expelled directly. The maximum pressure values recorded in this configuration are lower than in the previous case for small orifices, while for the larger ones are higher.

In Fig. 6 is presented the pressure time variation along the pipe for a relative orifice size of  $d/D = 0.128$  and a supply pressure of 4 bar.

The pressure recorded by transducers TP 4 and TP 5 (both placed initially in the air pocket) increases after the valve opening until the first pressure spike (caused by the impact of the water column with the pipe end). This suggests that the air compression is present in this case. In the same time, the acoustic effects can be observed in the pressure traces recorded inside the water column at TP 2 and TP 3 sections.

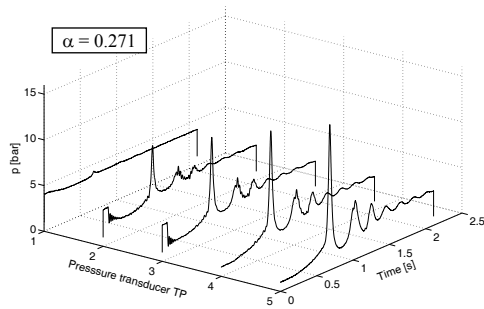


**Fig. 6. Pressure variation in time in case B,  $p_R = 4$  bar,  $d/D = 0.128$ .**

### 3.3 Configuration C

In this configuration, three pressure transducers are situated inside the air pocket (TP 3, 4 and 5) and the air pocket has the longest size  $\alpha = 0.4797$ . Similar to the previous cases, the compression of the air is more important for smaller orifices, and strongly decreases for the larger ones. For example, in case of the largest orifice ( $d/D = 0.374$ ), the compression is so reduced in the air pocket that before the first pressure spike the pressure increases by 2% for 4 bar supply pressure (Fig. 7). Also, the lumped gas mass hypothesis can be discussed, as TP 4 and 5 are simultaneously in the air pocket for half of the time of the water column displacement (until the water reaches TP 4).

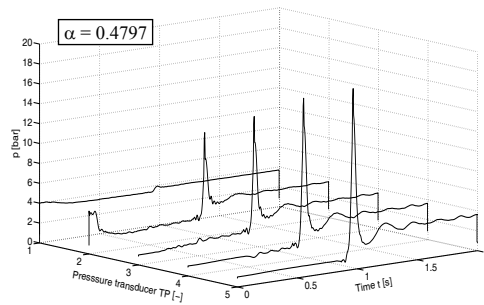


**Fig. 7. Pressure variation in time in case C,  $p_R = 4$  bar,  $d/D = 0.374$ .**

All the analysed situations of this configuration (of supply pressures and orifice sizes) showed that the pressure in the two measuring sections (TP 4 and 5) had the same amplitude and trace. This supports the assumptions made latter in the developed mathematical model that the pressure in the air pocket can be treated as a lumped gas mass (Lee, 2005).

### 3.4 Discussion between A, B and C configurations

Figure 8 presents the pressure recordings in TP5 section with a 5 mm diameter orifice and 4 bar supply pressure in all three tested air-water configurations. For the same value of the supply pressure, while the air pocket size increases, the maximum pressure decreases from 6 times the supply pressure in case A to 3 times in case C. For the presented cases, the oscillation period increases with the air pocket length, attributed to the presence

of an increasing amount of entrapped air (Lee, 2005). The apparition of the first pressure peak is delayed with the increase of the relative air pocket length, due to the longer distance for the water column to reach the pipe end.

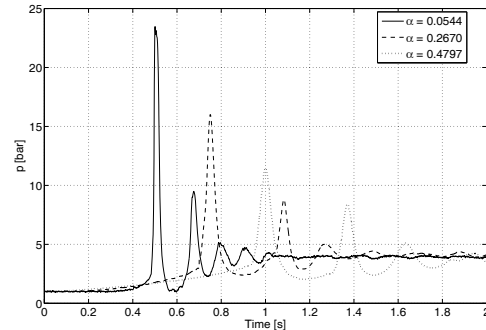


**Fig. 8. Relative air pocket length influence over the pressure at TP 5,  $d/D = 0.128$  and  $p_R = 4$  bar.**

The wave speed was determined from the time interval between two pressure spikes. The values obtained were in the following ranges: 125- 460 m/s for configuration A, 48-268 m/s for configuration B and 30 -166 m/s for configuration C. The values increase with the supply pressure and orifice size. For comparison, the wave speed in a Plexiglas pipe filled with flowing water is about 700 m/s, considering the experimental setup without air (wall thickness  $e = 10$  mm, bulk modulus for water  $K = 2.1$  GPa, and a Young modulus  $E_{\text{Plexiglas}} = 2.5$  GPa). The consistent difference between the values from air-water experiments and the theoretical one for full water flow, confirms that the wave speed decreases due to air entrapment (Wylie and Streeter 1993, De Martino *et al.* 2008).

The relative maximum pressure,  $p_{\text{max}}/p_0$ , at transducer TP5 (closest to the orifice) is presented in Fig. 9 as a function of the relative orifice size, for all three air pocket lengths.

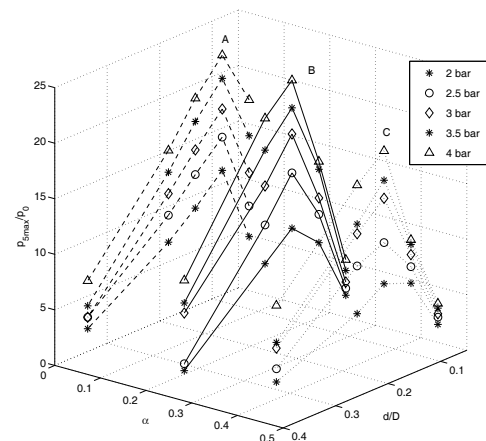


**Fig. 9. Relative maximum pressure measured in TP5 section (closest to the orifice) for configurations A, B and C.**

The maximum pressure depends essentially on the supply pressure and the orifice. In configuration A

(smallest air pocket), the highest maximum relative pressure at TP5 was recorded for a relative orifice diameter of 0.128, while in case B and C for 0.179. The results are similar to other experimental studies in the literature (Lee, 2005). For smaller orifices ( $d/D = 0.076, 0.128$ ), the maximum surge pressure decreases with the increase of the initial air pocket length. This decrease is attributed to the air compression observed in all cases for smaller orifices which has a cushioning effect according to previous studies (Zhou 2000, De Martino *et al.* 2008).

For larger orifices ( $d/D = 0.179, 0.230, 0.374$ ) the maximum surge pressure firstly increases with the increase of the initial air pocket length (from configuration A to B) and then decreases (from configuration B to C). In this case the orifice size was large enough to allow air evacuation without a significant compression (so no cushioning effect). The maximum surge pressure was caused by the water column impact at the pipe end, the water hammer phenomenon being dominant. The pressure decrease in configuration C compared to B is caused by larger head losses and a decrease of the pressure in the supply tank due to a longer pipe sector to fill with water. The maximum pressures were reduced in configuration A compared to B, because the distance between the valve and the pipe end was too short to allow flow acceleration, thus the developed inertia force of the flowing water column had a lower magnitude.

#### 4. MAXIMUM PRESSURE MODELLING

The above experimental results are similar to other results presented in the literature using a pipe steel (Zhou, 2000), and a Plexiglas pipe (Lee, 2005). A relation allowing determining the maximum pressure function of the system characteristics may be useful. Dimensional analysis and validation of the relations found are carried on for the experimental configuration ranges of air pocket length and orifice size.

##### 4.1 Dimensional Analysis

Analyzing the experimental data the following parameters were identified as having important influences over the transient phenomenon with expulsion of air: air pocket/water column configuration, orifice relative size,  $d/D$ , and initial supply pressure,  $p_R$ . In order to determine the dependence between the parameters above, a dimensional analysis is done, in which the following parameters are chosen:

- water properties: density,  $\rho$ , and dynamic viscosity,  $\mu$ ;
- system parameters: diameter,  $D$ , orifice diameter,  $d$ ;
- boundary conditions: flow velocity,  $v$ , water column length,  $L_w$  and air pocket size,  $L_a$ .

The wave speed is not chosen as a parameter of the model, because its determination is based on analysing recordings of pressure traces or

theoretical evaluation. The model is meant to predict the pressure surges in a simple manner. The wave speed influence is considered in the model constant. For the same purpose the pipe system parameters (friction, local losses and orifice discharge coefficient) are not evaluated and are considered in the model constant.

The effect of the initial pressure in the water column,  $p_R$ , is taken into account by including it in the water column velocity determination, according to the equation:

$$v = \sqrt{2(p_R - p_0)/\rho} \quad (2)$$

The maximum pressure during transients in a pipe that contains air pockets will be expressed as a function of dimensionless parameters that need to be determined. According Buckingham PI theorem, for 8 variables and 3 dimensions, 5 PI groups can be created. The following are chosen

$$\pi_1 = \frac{p_{\max}}{\rho v^2}; \pi_2 = \frac{d}{D}; \pi_3 = \frac{L_a}{L_w}; \pi_4 = \frac{D}{L_w}; \pi_5 = \frac{v D \rho}{\mu} = R \quad (3)$$

The maximum pressure may thus be expressed function of the other parameters such as

$$\frac{p_{\max}}{\rho v^2} = f\left(\frac{d}{D}, \frac{L_a}{L_w}, \frac{D}{L_w}, R\right) = k \left(\frac{d}{D}\right)^\beta \left(\frac{L_a}{L_w}\right)^\gamma \left(\frac{D}{L_w}\right)^\delta R^\epsilon \quad (4)$$

where  $k$  is a constant depending on the hydraulic characteristics of the set-up.

The above experiments showed that the variation of maximum pressure has a different pattern for 3 and 5 mm orifices ( $d/D = 0.076$  and  $0.128$ ) compared to the larger ones of 7, 9 and 15 mm ( $d/D = 0.179, 0.230$  and  $0.374$ ). In the first region, for the same orifice, the maximum pressure strongly decreases with the increase of the initial air pocket size. Contrary, it was observed that in the second region, the pressure first increases and then decreases with the air pocket size: the maximum values occur for case B (medium air pocket size), than for case C and last for case A. This is due to the different phenomena which are predominant in the transient flow development: air compression and water hammer, with or without entrapped air.

Considering the two variation tendencies, the recorded data of the maximum pressure were divided in two regions related to the orifice size and one equation was assumed for each region. The experimental data was fitted using the Matlab function *lsqnonlin*, a function designed to solve constrained linear least-squares problems.

For the orifices with a diameter of 3 and 5 mm ( $d/D = 0.076$  and  $0.128$ ), the following relation is obtained for the maximum pressure,  $p_{\max,1}$ :

$$\frac{p_{\max,1}}{\rho v^2} = 4.9 \cdot 10^7 \left(\frac{d}{D}\right)^{1.77} \left(\frac{L_a}{L_w}\right)^{-0.37} \left(\frac{D}{L_w}\right)^{0.37} R^{-0.84} \quad (5)$$

In case of the orifice with a 7 mm diameter and larger ( $d/D \geq 0.179$ ), the maximum pressure,  $p_{\max,2}$  is evaluated using the equation:

$$\frac{p_{\max,2}}{\rho v^2} = 0.16 \left(\frac{d}{D}\right)^{-1.25} \left(\frac{L_a}{L_w}\right)^{0.3} \left(\frac{D}{L_w}\right)^{-1.49} R^{-0.46} \quad (6)$$

In order to choose the equation to model the maximum pressure, a criterion, *krit*, was derived from the intersection of Eqs. (5) and (6)

$$krit = 3.27 \cdot 10^{-9} \left(\frac{d}{D}\right)^{-3.02} \left(\frac{L_a}{L_w}\right)^{0.67} \left(\frac{D}{L_w}\right)^{-1.86} R^{0.38} \quad (7)$$

If *krit* is equal to or over 1, the first equation, Eq. (5) is applied for maximum pressure computation, else the second equation, Eq. (6) is used.

Both Eqs. 5 and 6 show the importance of the flow velocity and the supply pressure in the amplitude of the maximum pressure. The equations also confirm the experimental observations; the maximum pressure first increases with the increase of the orifice diameter, and after a critical value, decreases, as the exponent of *d/D* is positive in Eq. (5) and negative in Eq. (6).

In the first region with lower values of orifice size, the influence of the air compression is more significant than in the second one. Here, the maximum pressure decreases with the increase of the air pocket size, *L<sub>a</sub>*, because of the orifice incapacity to totally evacuate the air. The remaining air has a cushioning effect which increases with *L<sub>a</sub>*. In the second region, for the same *L<sub>a</sub>*, more air is evacuated as the orifice is larger. The air is less compressed, and the inertia of the water column, *L<sub>w</sub>*, is more important in the amplitude of the maximum pressure, like in Eq. 6.

The prediction of the maximum pressure was first obtained using Eqs. (5) and (6) with the flow velocity determined as a function of the supply pressure. Second, a similar model was created using estimated flow velocities determined by considering the distance travelled by the water column (equal to the air pocket length) divided by the time interval between valve opening and the impact moment with the pipe end. Results are presented for all three sizes of the air pocket (Fig. 10).

The values in Fig.10 are ordered after the orifice diameter (3, 5, 7, 9 and 15 mm) and for each orifice the supply pressure is set in an increasing order (e.g. samples 1, 2 and 3 correspond to 3 mm orifice at 2, 3 and respectively 4 bar supply pressure). It can be seen that using both versions of the model (with a measured velocity and with a computed velocity) the results follow the experimental data trend.

The largest differences can be found at samples 3 and 6 in the smallest air pocket (case A), for the results obtained using the computed velocity as a function of supply pressure. They correspond to 4 bar supply pressure with 3 and 5 mm orifices (*d/D* = 0.076 and 0.128). This is due to the model simplicity, which does not take into account the effect of entrapped air or air compression. These two phenomena were especially observed in these cases, so the differences between the model results and the experiments are considered motivated.

As the pressure evaluation using the flow velocity obtained in function of the supply pressure is satisfactory, the velocity determined with Eq. (2) will be used further in the model.

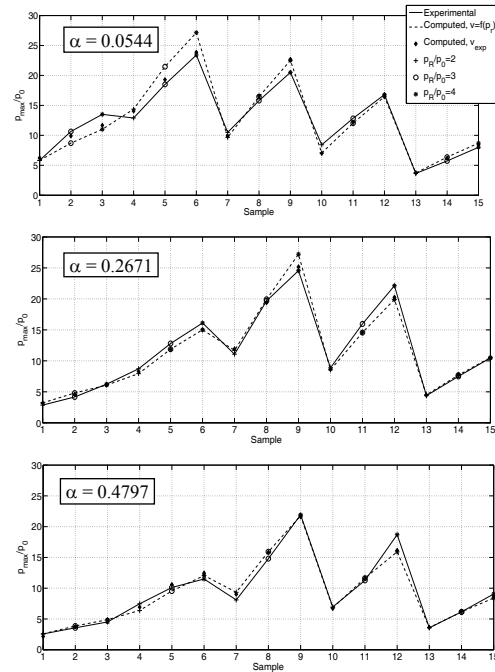


**Fig. 10. Comparison between measured and computed values of the maximum pressure.**

## 4.2 Test Validation

The validation of the proposed model was realized in two stages, with additional data from the experiments unused in the determination of the equations coefficients and with two sets of experimental data available in the literature in the same range of configurations (Table 2).

**Table 2 Characteristics of experimental set-ups used for validation**

Set-up	$\alpha$	$p_R/p_0$	$d/D$
Present	0.0544	2.5	0.076
	0.2671		0.128
	0.4797	3.5	0.179
			0.230
			0.374
Lee (2005)	0.195	2	0.06
	0.335	3	0.121
	0.448	4	0.183
			0.244
			0.366
Zhou (2000)	0.2	4.57	0.057
			0.114
			0.142
			0.171
			0.2
			0.257
			0.342
			0.428

First, experimental results from the set-up of the present paper were used, obtained for intermediate supply pressures of 2.5 and 3.5 bar (Fig. 11, e.g.

samples 1 and 2 correspond to 3 mm orifice at 2.5 and 3.5 bar supply pressure). It can be noticed that sample 4 from A case, which has the largest difference, corresponds to a 5 mm orifice diameter ( $d/D = 0.128$ ) at a high supply pressure (3.5 bar). This may be due to an underestimation of the air compression phenomenon, as in the previous analysed cases.

For the second validation stage, experimental data available in the literature obtained for a Plexiglas pipe, Lee (2005), and a steel pipe, Zhou (2000), are used. The laboratory set-ups and the tested configurations are chosen to have approximately the same geometrical characteristics (Table 2). The total pipe lengths vary up to 33%, while the pipe diameters are smaller than the one used in the present work (Plexiglas - 33% and steel - 10%). The relative parameters are in the same range for the tested configurations.

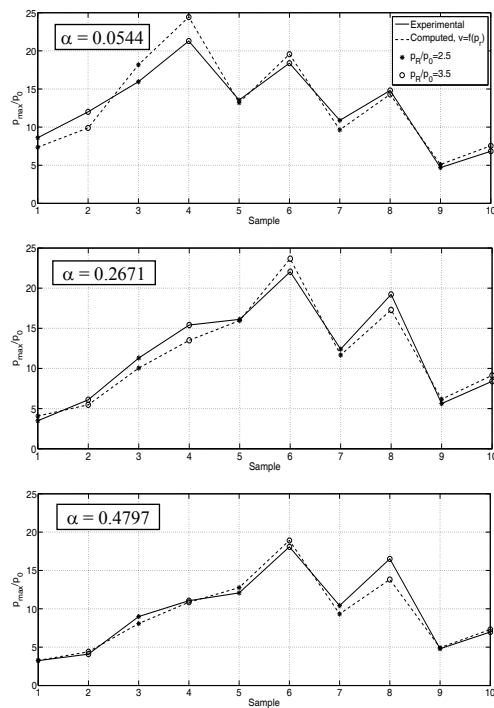


**Fig. 11. Validation of the maximum pressure obtained in the present experimental set-up, for 2.5 and 3.5 bar supply pressure.**

Because of the limited information, the hydraulic losses of each set-up in the literature (Lee 2005, Zhou 2000) are included in the computation models as constants characteristics of the installation. The constants are determined in order to obtain the best fitting between the measured and computed values and are chosen as follows:

- Lee (2005):  $k_{1L} = 3.185 \cdot 10^7$  and  $k_{2L} = 0.056$ ;
- Zhou (2000):  $k_{1Z} = 9.31 \cdot 10^7$  and  $k_{2Z} = 0.28$ .

The results for the Plexiglas pipe of Lee (2005) are presented in Fig. 12. Generally, the trend of pressure variation is closely simulated and many of the maximum pressure values are well approximated. The most significant differences are

found at samples 4-6 which correspond to a small orifice,  $d/D = 0.121$ . According to Lee (2005), in this case of orifice relative size, entrapped air presence had a considerable amplifying effect. So it can be considered that these differences are also due to the model simplicity, as in the present experimental data modelling.

It can be seen in Lee (2005) experimental results the same maximum pressure variation between the analysed cases as in the present experiments. For the smaller orifices the maximum pressure strongly decreases with the increase of the initial air pocket size. For larger orifices the pressure first increases and then decreases with the air pocket size. This is also related to the different phenomena which are predominant in the transient flow development: air compression and water hammer, with or without entrapped air.

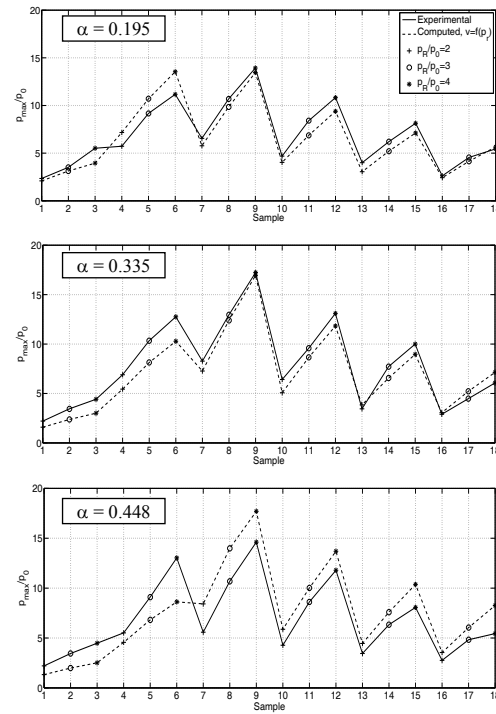


**Fig. 12. Maximum pressure measured by Lee (2005) and computed for Plexiglas pipe.**

The last validation involves the experimental and numerical results obtained by Zhou (2000) in a steel pipe with the characteristics presented in Table 2. It can be seen that the pressure surges are higher than in the previous presented works, up to 15 times the supply pressure (Fig. 13). This can be set on the higher Young modulus for steel ( $E_{steel} = 200$  GPa) than for Plexiglas ( $E_{Plexiglas} = 2.5$  GPa). The trend of the maximum pressure variation is well captured by the present model, being able to consider the influence of different characteristics of the set-ups and of the pipe materials. The most important differences between the computed values and the experiments are also in the relatively small orifices region, due to the model simplicity which is not considering the air compression and entrapped air effects.

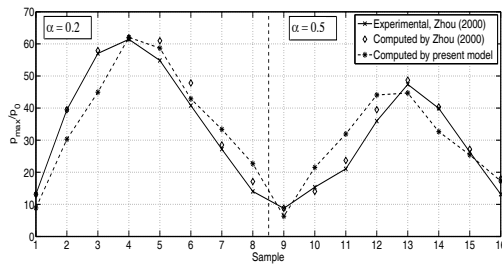


**Fig. 13. Maximum pressure measured and computed by Zhou (2000) and validated for the steel pipe.**

## 5. CONCLUSIONS

A detailed experimental analysis of the transient flow in a horizontal pipe containing an air pocket was done on a laboratory set-up. The tests were realized for a wide range of configurations of water column length, air pocket size, supply pressure and orifice diameter. Two different variation patterns of the pressure surges were observed, for smaller orifices the air compression being predominant and for larger orifices the water hammer phenomenon. In some cases, the entrapped air presence had an important influence over the maximum pressures. The results confirmed previous results available in the literature.

Dimensional analysis and experimental data were used to determine the relation between the main parameters influencing the phenomenon, in order to estimate the maximum pressure with minimum details of the hydraulic system and its operation regime. A two equations model comprising a criterion was derived for the present experimental configurations range ( $\alpha = 0.05 - 0.48$ ,  $d/D = 0.07 - 0.38$ ,  $p_R/p_0 = 2 - 4$ ) and a large amount of experimental data was used to achieve a good fitting of the results. As the model does not explicitly consider the air compression and entrapped air effects, some limitations for maximum pressure evaluation in the range of relatively small orifices are present.

The validation of the two equations model was done with additional experimental data of the present set-up and using data available in the literature obtained in a Plexiglas pipe and a steel pipe, having similar configuration with the one used in the present work.

The model captured the variation trend of the maximum pressure in all analysed situations, considering only general information about geometrical and operational characteristics, and the constants characteristics of the set-ups introduced for fitting. Still, there are some differences in the correct evaluation of the maximum pressure values for some particular cases due to importance of the air compressibility and entrapped air effects. A more precise evaluation should include in the modelling the influence of these effects. Also, for generalization, the determination of the set-ups characteristics constants has to be done. All the aspects mentioned above are subjected for the future researches.

## ACKNOWLEDGEMENTS

The work has been funded by the Sectoral Operational Programme Human Resources Development 2007-2013 of the Ministry of European Funds through the Financial Agreement POSDRU/159/1.5/S/134398 and by the Executive Agency for Higher Education, Research, Development and Innovation, PN-II-PT-PCCA-2013-4, no. 88/2014 ECOTURB Project. Also, the presented research was carried out as a part of "Swedish Hydropower Centre-SVC". SVC has been established by the Swedish Energy Agency, Elforsk and Svenska Kraftnät together with Luleå University of Technology, KTH Royal Institute of Technology, Chalmers University of Technology and Uppsala University.

## REFERENCES

- Carlos, M., F. J. Arregui, E. Cabrera and C. V. Palau (2011). Understanding Air Release through Air Valves. *Journal of Hydraulic Engineering* 137(4), 461-469.
- Cheng, Y., J. Li and J. Yang (2007). Free surface-pressurized flow in ceiling-sloping tailrace tunnel of hydropower plant: Simulation by VOF model. *J. Hydraul. Res.* 45(1), 88-99.
- De Martino, G., N. Fontana and M. Giugni (2008). Transient Flow Caused by Air Expulsion through an Orifice. *Journal of Hydraulic Engineering* 134(9), 1395-1399.
- Environmental Hydraulics Group (1996). Hydraulic Transient Evaluations of the City of Edmonton Sewage system. *Consulting report* prepared for the City of Edmonton, Environmental Hydraulics Group.
- Gjerde R. U. (2009). *Air Problems in water intake. Air lift model and application on water intake Holmaliåna*. Master thesis, Norwegian University of Science and Technology, Trondheim, Norway [in Norwegian]
- Izquierdo, J., V. S. Fuertes, E. Cabrera, P. L. Iglesias and J. García-Serra (1999). Pipeline start-up with entrapped air. *Journal of Hydraulic Research* 37(5), 579-590.
- Lauchlan, C. S., M. Escameia, R. W. P May, R. Burrows and C. Gahan (2005). Air in pipelines. A literature review. *HR Wallingford Ref: SR649*
- Lee, N. H. (2005). *Effect of pressurization and expulsion of entrapped air in pipelines*. Ph. D. thesis, Georgia Institute of Technology, Georgia, United States.
- Lee, T. S., H. T. Low and D. T. Nguyen (2008). Effects of air entrainment on fluid transients in pumping systems. *Journal of Applied Fluid Mechanics* 1(1), 55-61.
- Liou C. P. and W. A. Hunt (1996). Filling of pipelines with undulating elevation profiles. *Journal of Hydraulic Engineering* 122(10),

- 534–539.
- Liu, D. and L. Zhou (2009). Numerical simulation of transient flow in pressurized water pipeline with trapped air mass. In *Proceeding of Power and Energy Engineering Conference. APPEEC. Asia-Pacific*, Wuhan, China. 104-107.
- Pitorac, L. I., D. M. Bucur, D. Dunca and M. J. Cervantes (2016). Modelling Transient Multiphase Flow in Pipeline. *UPB Scientific Bulletin, Series D: Mechanical Engineering* 78(2), 179-188.
- Schafer, R. W. (2011). On the frequency-domain properties of Savitzky-Golay filters. In *Proceeding of Digital Signal Processing Workshop and IEEE Signal Processing Education Workshop (DSP/SPE)*. IEEE, Sedona, Arizona USA
- Tatu, G. (1999). Unsteady flow in HPP intakes caused by air pockets expulsion, *Pressurized Hydraulic Systems Conference*, 17-19 June 1999, 192-200, Bucharest, Romania [in Romanian]
- Wylie, E. B. and V. L. Streeter (1993). *Fluid transients in systems*. Prentice-Hall, Englewood Cliffs, N.J.
- Zhou F. (2000). *Effects of Trapped Air on Flow Transients in Rapidly Filling Sewers*. Ph. D. thesis, Dep. for Civil and Environmental Engineering, Edmonton, Alberta
- Zhou, F., F. Hicks and P. Steffler (2004). Analysis of effects of air pocket on hydraulic failure of urban drainage infrastructure. *Canadian Journal of Civil Engineering* 31(1), 86-94.
- Zhou, L., D. Liu, B. Karney and Q. Zhang (2011). Influence of Entrapped Air Pockets on Hydraulic Transients in Water Pipelines. *Journal of Hydraulic Engineering* 137(12), 1686-1692.